



Published in final edited form as:

J Hazard Mater. 2009 May 30; 164(2-3): 1074–1081. doi:10.1016/j.jhazmat.2008.09.003.

The Impact of Composition on the Physical Properties and Evaporative Mass Transfer of a PCE-Diesel Immiscible Liquid

Kenneth C. Carroll^{1,2}, Renee Taylor², Evan Gray², and Mark L. Brusseau^{1,2,*}

¹Department of Soil, Water and Environmental Science, University of Arizona, 429 Shantz Building #38, P.O. Box 210038, Tucson, Arizona 85721-0038, United States

²Department of Hydrology and Water Resources, University of Arizona, Harshbarger Building #11, Tucson, Arizona 85721-0038, United States

Abstract

The impact of immiscible-liquid composition on mass transfer between immiscible liquid and vapor was evaluated for a complex mixture of chlorinated solvents and petroleum hydrocarbons. A mixture of PCE (tetrachloroethene) and diesel was discovered at a site in Tucson, Arizona. Partitioning of PCE into a previously spilled diesel free product has been observed, with resultant concentrations of PCE above 15% by weight. The density, viscosity, surface tension, and interfacial tension were measured for PCE-diesel mixtures with PCE fractions from 7 to 32%, and the results indicated that immiscible-liquid composition did impact the physical properties of the PCE-diesel mixture. Comparison of gas and aqueous phase partitioning results to predictions based on Raoult's Law indicated that the immiscible liquid behaved essentially as an ideal mixture. Flow-cell experiments were conducted to characterize PCE removal from the PCE-diesel mixture via vapor extraction. The effluent concentrations for the experiment conducted with free-phase immiscible liquid were comparable to equilibrium values. Conversely, they were significantly lower for the experiment wherein a residual saturation of immiscible liquid was distributed within sand. These results suggest that evaporation for the latter experiment was constrained by rate-limited mass transfer, which was attributed to dilution effects associated with a nonuniform immiscible-liquid distribution.

Keywords

SVE; Diesel; PCE; multicomponent immiscible liquid; Raoult's Law

1. Introduction

Complex multicomponent immiscible liquids are present at many hazardous waste sites, and significantly complicate contamination characterization and remediation [1,2]. The design of effective remediation operations for such systems necessitates an understanding of the immiscible-liquid composition and its impact on contaminant mass removal. Mass transfer from multicomponent immiscible liquid can be nonideal due to compositional issues, including mole-fraction associated constraints and nonideal mixture behavior [1-9], or mass-transfer rate limitations [10-13].

Previous research evaluating the compositional evolution of multicomponent immiscible liquid during evaporation or volatilization has been limited to date [2,13-17]. Both aqueous and vapor flushing may alter the chemical composition of the immiscible-liquid mixture by preferentially

*Corresponding author (Brusseau@ag.arizona.edu).

extracting high solubility [18] or volatility [13] compounds, which may affect the ideality of the mixture [1]. These compositional changes could also affect the density of the mixture, as well as alter other physiochemical properties such as interfacial tension and viscosity [19]. There have been relatively few investigations of rate-limited mass transfer between multicomponent immiscible liquid and gas phases in porous media under dynamic conditions [2,13-17]. For example, Harper et al. [16] compared single, two, and four component immiscible-liquid mixtures, and observed significant variability in mass-transfer rate limitation with immiscible-liquid composition.

The purpose of this investigation was to evaluate the effects of PCE-diesel mixture composition on physical properties of the mixture, and on PCE evaporation. The immiscible liquid evaluated herein was a PCE-diesel mixture present at a hazardous waste site in Tucson, Arizona. The impact of PCE content on physical properties of the immiscible liquid was investigated. The evaporation behavior of PCE was examined with a series of batch and flowcell experiments.

2. Materials and Methods

2.1. Site Description

The Park-Euclid Site is a Water Quality Assurance Revolving Fund (or Arizona State Superfund) Site located in Tucson, Arizona [20]. A dual-phase extraction and treatment system is currently being installed to remediate the vadose zone and shallow groundwater, which is contaminated with diesel compounds and volatile organic compounds including PCE, trichloroethene (TCE), and cis-1,2 dichloroethene. A separate immiscible-liquid phase comprised of diesel fuel free product is present near the top of the perched water-bearing unit at the site. The partitioning of PCE into the diesel has formed a complex immiscible-liquid mixture. The presence of elevated PCE concentrations in the immiscible liquid is a concern for remediation efforts.

2.2. Immiscible-Liquid Mixtures

A sample of the PCE-diesel free product present at the Park Euclid site was collected with a Teflon well bailer, and stored at 4 degrees Celsius ($^{\circ}\text{C}$) in amber glass vials (VWR, Brisbane, CA) with Teflon lined caps. A subsample of the original immiscible-liquid mixture was sent to Transwest Geochem Laboratories (Scottsdale, AZ) for chemical analysis and characterization using GC-MS. The concentration of PCE in the original immiscible-liquid mixture was determined to be $72,000 \text{ mg Kg}^{-1}$, and this was used as the initial (lowest) PCE concentration for the experiments. Four additional subsamples with larger PCE concentrations were then created by adding known amounts of PCE (99% ACS Grade, Acros Chemical Company, New Jersey) to subsamples of the original immiscible-liquid mixture, resulting in PCE compositions ranging from 7.2% to 32% by weight (72,000; 118,206; 169,360; 232,814; and $320,942 \text{ mg Kg}^{-1}$ PCE in immiscible liquid). For comparative purposes, a simple two-component immiscible-liquid mixture was created by mixing PCE (15% by weight) and hexadecane (99% ACS Grade, Acros Chemical Company, New Jersey).

2.3. Physical Property Measurements

Physical property measurements including density, viscosity, and interfacial and surface tensions were conducted for the immiscible-liquid mixture to characterize the effect of PCE. Measurements were also made for the two-component liquid, pure PCE (99% PCE), and pure hexadecane (0% PCE). All fluids were kept in a constant temperature bath, and experiments were performed at $25(\pm 2)^{\circ}\text{C}$. Immiscible-liquid volumes were prepared in 5 ml volumetric flasks (Kimble-Kontes, Vineland, New Jersey) and masses of the fluids were determined gravimetrically using an analytical balance (Mettler Toledo PG-S, Greifensee, Switzerland). These measurements were conducted in triplicate, and the density of distilled-deionized

NANOpure (Series 550, Barnstead Thermolyne Corp., Dubuque, Indiana) water was also measured to confirm method accuracy. Viscosity measurements were conducted using a Gilmont Instruments Size #1 (0.2 and 10 centipoise range) Falling Ball Type Viscometer obtained from VWR (Brisbane, CA). The time of decent required for the ball to fall a specified distance imprinted on the viscometer tube was measured with a stop-watch up to five times to examine the experimental variability. The viscosity of NANOpure water and hexadecane were used to calibrate the instrument, and measurements were then made for the various immiscible-liquid mixtures.

The surface and interfacial tension for each of immiscible-liquid mixtures were measured using a Fisher Surface Tensiomat Model 21 (Fisher Scientific International, Inc., Atlanta, GA), following the principles of operation specified by the American Society for Testing Materials in Methods D-971 (interfacial tension of oil against water) and D-1331 (surface and interfacial tensions of detergents). The instrument uses the du Nouy ring-method, which employs a platinum-iridium ring of precisely known dimensions suspended from a counter-balanced lever arm. Clear glass 50 ml beakers (Kimble-Kontes, Vineland, New Jersey) were cleaned with dichloromethane, then acetone, an acid bath, and NANOpure water before oven drying prior to each use. The platinum-iridium ring was cleaned first with dichloromethane and then with acetone, which was allowed to evaporate prior to each measurement. The tensiostat was calibrated before every surface and interfacial tension measurement to the surface tension of NANOpure water to confirm the accuracy of the dial reading. Measurements were made with NANOpure water equilibrated with the immiscible-liquid mixture used. Interfacial tension measurements were made from the more dense liquid to the less dense liquid by exerting an upward force on the ring, and breaking the interface as the ring is displaced from the lower (denser) liquid to the upper (lighter) liquid.

2.4. Batch Experiments

Batch experiments were conducted to characterize PCE evaporation and dissolution. The experiments utilized each of the PCE-diesel mixtures in triplicate. The phase partitioning experiments were conducted at 25(±2)°C with glass vials (VWR Trace-Clean 25 ml vials with open top caps and Teflon lined septa, Brisbane, CA). Immiscible liquid was extracted from the containers with a Gastight Hamilton Company syringe (Reno, Nevada), and added to the vials. NANOpure water was added to the appropriate immiscible-liquid/aqueous vials, and the mass of the water added to each vial was measured with an analytical balance (Mettler Toledo PG-S, Greifensee, Switzerland). The vials were then placed on an Orbit Model shaker table (Lab-Line Instruments, Inc., Melrose Park, Illinois) set to 200 RPM for 120 hours to ensure complete equilibration, and then centrifuged (Beckman GP Centrifuge, Palo Alto, CA) at 2000 RPM for 30 minutes to effect phase separation. Then aqueous or gas phases were collected from the vials with a Gastight Hamilton Company syringe inserted through the Teflon septa of the vials. The sub-samples were analyzed for PCE, and statistical confidence intervals (95% C.I.) were calculated from the triplicates.

2.5. Flow Cell Experiments

Two nearly identical two-dimensional (2D) flow cells were used for dynamic vapor extraction experiments. The inner dimensions of the flow cells were approximately 5.3 centimeters (cm) by 19.9 cm by 39.7 cm (Table 1). The basic construction consisted of a 1/16 inch (0.16 cm) stainless-steel sheet that was cut and welded into a rectangle to the dimensions described above with an approximately 1 inch (2.54 cm) flange lined with a PTFE flange gasket (TEADIT Intl., supplied by McMaster-Carr, Los Angeles, CA) to seal the frame to a 3/8 inch (0.95 cm) tempered glass plate. Four inlet/outlet ports were placed at each end to allow vapor injection and extraction. A 0.2 µm diffusion plate (Mott Metallurgical Corp., Farmington, CT) was welded onto the inside of each of the ends. The influent, effluent, and sampling ports (along a

vertical transect in the back flow cell) were installed with 1/8 inch (0.32 cm) VICI Septum Injector Nuts containing 1/4 inch (0.64 cm) Teflon lined septa (Valco Instruments Co. Inc., Houston, TX) for sample collection of vapor effluent and vapor and immiscible liquid within the flow cell. A Swagelok sampling port, a cold trap, a flow meter, a moisture trap, and a carbon filter were connected to the effluent tubing.

One of the experiments was conducted without porous media packed in the flow cell (including only free-phase immiscible liquid, water, and mobile vapor phase). After a leak test, 2,300 ml of water were injected into the back port, 650 ml of the PCE-diesel were injected above the water, and the remainder of the flow-cell volume contained the mobile gas phase. The system was designed so that samples of each fluid phase could be collected using ports located at the back of the flow cell. The other flow cell was packed with uniform fine-grained sand (0.68 mm median grain size, 20-30 mesh Accusand, Unimin, Canada), and also contained water, immiscible liquid, and a mobile gas phase. The sand was wet packed to a bulk density of 1.84 g cm⁻³ and porosity of 0.32, and then the flow cell was saturated with nitrogen sparged NANOpure water from the bottom with a Gilson 305 HPLC piston pump (Gilson Medical Electronics, Middleton, WI) at a flow rate of 0.25 ml min⁻¹ until a constant flow cell mass was achieved.

The original immiscible liquid collected from the site was used in both flow cell experiments. The immiscible liquid was introduced into the porous-medium packed flow cell from the top using a gas-tight syringe (SGE Intl. Pty. Ltd., Ringwood, Australia) attached to a syringe pump (Sage Instruments 355 syringe pump, Orion Research Inc., Boston, MA). The ports at the bottom of the flow cell were left open to allow the water in the flow cell to drain freely. Water saturated with the immiscible-liquid components was then pumped into the flow cell at 0.5 ml min⁻¹ for approximately 3 days from the top to distribute the immiscible liquid within the flow cell. In total, 736 ml of water were displaced, but none of the immiscible liquid was extracted from the flow cell. The flow cell was then desaturated with the injection of immiscible-liquid equilibrated gas. The desaturation mobilized 69.5 ml of the immiscible liquid, which was removed during the process.

A single high performance vacuum pump (RobinAir CoolTech model 15600, 6 cfm capacity, RobinAir, SPX Corp., Montpelier, OH) with an in-line flow meter (Gilmont model F1100, Gilmont Instruments, Barrington, IL) was used to simultaneously extract vapor through both flow cells. The pump created a relatively constant flow rate that produced similar discharge from each flow cell (Table 1). Effluent vapor samples were collected periodically for analysis of PCE. In addition, gas, aqueous phase, and PCE-diesel phase samples were collected for compositional analysis before the start and at the end of the experiment conducted with free-phase immiscible liquid. The gas phase sampling involved collection of 50 ml of gas from the port located above the immiscible liquid. The sample was injected into a Tedlar sample bag, which was then sealed, placed on ice, and shipped overnight to Transwest's laboratory for analysis. The PCE-diesel phase was collected from a port on the back of the flow cell using a gas-tight syringe inserted through a Teflon-lined septum nut. The immiscible liquid was injected into a 2 ml amber-glass volatile organic analysis vial (National Scientific Co., Quakertown, PA).

2.6. Chemical Analysis

Subsamples of the immiscible liquid collected from the field were analyzed using gas chromatography-mass spectroscopy (GC-MS) to characterize the immiscible-liquid composition. The analyses, conducted by Transwest Geochem Laboratories (Scottsdale, AZ), consisted of EPA Methods 8260 and 8270 following extraction with hexadecane. In addition, method EPA Method 8015 was used to provide a combined-total concentration for groups of molecules with similar structures and molecular weights by integration of sections of the GC-

MS chromatogram. These groups represent the molecules of common carbon chain length from 9 – 25 (with negligible concentrations besides PCE and TCE below 9 carbons and above 25).

Samples from the batch and flow cell experiments were analyzed using GC flame ionization detection (FID) (Shimadzu, Japan) to determine the concentration of PCE in gas and water samples. Analytical standard solutions were prepared from reagent-grade PCE (99.9% Aldrich), reference samples were analyzed every 5-6 samples to monitor changes in the GC system, and the quantifiable detection limit was approximately 0.03 mg L^{-1} . Aqueous phase samples were prepared by adding 5 ml of the sample into a headspace vial (Kimble) sealed with open caps and Teflon-faced septa. The gas samples (1 ml) were injected into capped headspace vials that contained 5 ml of water.

3. Data Analysis

3.1. Partitioning and Raoult's Law

For both vapor and aqueous phase systems, the ideality of the partitioning was evaluated by comparing measured concentrations to those predicted from Raoult's Law [1,21-23]:

$$S_A = S_A^o X_N \quad (1)$$

where the subscripts $_A$ refer to air (vapor phase) or aqueous phase and $_N$ refer to immiscible liquid; superscript o signifies the pure phase (single component); S_A is the concentration of the component in gas or water; S_A^o is the pure compound solubility or vapor concentration; X_N is the mole fraction of the compound in the immiscible liquid. Raoult's Law has been used to predict aqueous concentrations of compounds for many immiscible-liquid mixtures [5,18,21, 22,24-37]. The mole fractions (X_{Ni}) for specific components of the mixtures were calculated with:

$$X_{Ni} = \frac{\left(\frac{C_{Ni}}{MW_i} \right)}{\sum \left(\frac{C_{Ni}}{MW_i} \right)} \quad (2)$$

where C_{Ni} is the mass of an immiscible-liquid component per mass of sample, MW_i is the molecular weight of each component. C_{Ni} is obtained by GC-MS chemical analysis of the immiscible-liquid mixture as described above.

3.2. Mass Transfer Kinetics

Evaporation of compounds from immiscible liquid to the gas phase is typically conceptualized as diffusion from the interphase boundary using a linearized form of Fick's law for mass-transfer kinetics [10,38]:

$$J = k_f a_o (C_s - C) = k_o (C_s - C) \quad (3)$$

where J is the mass-transfer rate per unit volume of immiscible-liquid component between the phases; a_o is the specific interfacial area; k_f is the mass-transfer coefficient; k_o is the lumped mass-transfer coefficient; C_s is the concentration of the immiscible-liquid component in the

vapor phase at equilibrium with the immiscible liquid; and C is the bulk vapor-phase concentration of the immiscible-liquid component. The lumped mass-transfer coefficient is generally used due to the difficulties of measuring immiscible-liquid/vapor interfacial areas. The lumped mass-transfer coefficient may be estimated at quasi-steady state assuming negligible dispersive flux:

$$k_o = -\left(\frac{q}{L}\right) \ln\left(1 - \frac{C}{C_s}\right) \quad (4)$$

where q is the mobile phase Darcy velocity and L is the source length. The above equation was used to estimate the lumped PCE-evaporation rate coefficient based on effluent concentrations from the vapor extraction experiments.

Correlations of mass-transfer kinetics using the modified Sherwood number and the Peclet number have been used to evaluate interphase mass transfer from immiscible liquid to the vapor phase [10-12]. The modified Sherwood number is defined as:

$$Sh_m = \frac{k_o (d_{50})^2}{D} \quad (5)$$

where d_{50} is the median grain size of the porous media (characteristic length) and D is the mobile phase diffusion coefficient for an immiscible-liquid component [10,39]. One half of the immiscible-liquid height (1.5 cm) was used for the characteristic length (instead of the median grain size) for the flow cell experiment conducted without porous media. The Peclet number is defined as:

$$Pe = \frac{v d_{50}}{D} \quad (6)$$

where v is the interstitial (pore) velocity for the mobile gas phase. The correlation developed by Wilkins et al. [10] is:

$$Sh_m = 10^{-2.79} Pe^{0.62} \left(\frac{d_{50}}{0.05}\right)^{1.82} \quad (7)$$

or

$$k_o = 10^{-0.42} D^{0.38} v^{0.62} d_{50}^{0.44} \quad (8)$$

which was developed for a variety of grain sizes, and is similar to the correlation presented in Yoon et al. [11] for variable grain sizes and water contents. Estimated PCE evaporation-rate coefficients from the PCE-diesel immiscible liquid from the vapor extraction experiments were compared to values produced with the Wilkins et al. [10] correlation.

3.3. Mobilization Potential

Immiscible-liquid mobilization potential has generally been evaluated in terms of the capillary and bond numbers. The capillary number is the ratio of the viscous force to the capillary force [40-43]. The capillary number (N_{Ca}) is:

$$N_{Ca} = \frac{k\rho g \Delta H}{\gamma} = \frac{v\mu}{\gamma} \quad (9)$$

where k is the porous medium intrinsic permeability, g is gravitational acceleration, ΔH is the hydraulic head gradient, v is the groundwater velocity, μ is the aqueous viscosity, and γ is the interfacial tension. Larson et al. [44] measured N_{Ca} values for various flow rates and found that immiscible-liquid displacement began at N_{Ca} of 2×10^{-5} .

The Bond number represents the ratio of gravitational forces to capillary forces that affect fluid trapping and mobilization [45]. The bond number (N_{Bo}) is:

$$N_{Bo} = \frac{\Delta\rho g k}{\gamma} \quad (10)$$

where $\Delta\rho$ is the density difference between the immiscible fluids, g is gravitational acceleration, and k is the intrinsic permeability [43]. Assumptions, including a homogeneous, isotropic hydraulic conductivity of 30.4 ft day^{-1} (obtained from an aquifer test report [46]), and a uniform hydraulic gradient of 0.008 measured from water level data were used to estimate groundwater velocity and aquifer permeability [20].

4. Results and Discussion

4.1. PCE-Diesel Mixture Composition

The results of the chemical analysis of the immiscible-liquid mixture collected from the field are presented in Table 2, along with the mole fractions of the mixture components. The components identified in the GC-MS analysis accounted for approximately 90% of the total immiscible liquid composition. The remaining ~10% was approximated by the average molecular weight of diesel (227 g mol^{-1}) as reported in the literature [6,26,27]. The original PCE-diesel mixture contained PCE, TCE, and a range of compounds with a mean carbon chain length of C17, with decreasing concentrations for higher and lower carbon chain lengths. The composition and mole fractions determined after subjecting the immiscible liquid to vapor extraction are also presented in Table 2.

4.2. Immiscible liquid Physical Properties

The measured densities and viscosities for the PCE-diesel mixtures are presented in Figure 1a. As expected, the immiscible-liquid mixture density increased with increasing PCE concentration. The measured densities of PCE (1.6 g cm^{-3}) and hexadecane (0.773 g cm^{-3}) were comparable to published values [47]. The change in both density and viscosity were linear functions of PCE concentration. The immiscible liquid transitioned from being less dense than water to denser than water when PCE concentrations exceeded approximately 26% by weight (Figure 1a). The immiscible-liquid mixture viscosity decreased with increasing PCE concentrations, which was also expected. Both of the trends for density and viscosity suggest that immiscible-liquid mobility potential increased with PCE concentration.

The surface and interfacial tension measurement results are shown in Figure 1b. The immiscible-liquid surface tension remained relatively constant over the measured PCE composition range for both the PCE–diesel mixtures and the two-component immiscible-liquid mixture. The measured surface tension of hexadecane (27 dyn cm^{-1}) was comparable to a published value [47]. The interfacial tension values for the PCE–diesel mixture are reduced relative to pure hexadecane (46 dyn cm^{-1}) and pure PCE (37 dyn cm^{-1}), and followed a linear trend of decreasing tension with increasing PCE concentration. The diesel fraction of the mixture contains compounds that differ significantly from hexadecane, and it is possible that the more-polar diesel compounds may have partitioned to the immiscible-liquid interface, causing the lower interfacial tension. The observed decrease in interfacial tension with increased PCE concentration is another factor that may increase potential for immiscible-liquid mobility.

The calculated capillary and bond numbers for the PCE-diesel immiscible-liquid mixtures are shown in Figure 1c. The bond number increased with increasing PCE concentration due to an increase in the gravitational force and a decrease in capillary force due to PCE additions. The sample with the highest PCE concentration became a dense immiscible liquid, and the bond number became positive. Capillary numbers also increased with increasing PCE concentrations, due to the decreased capillary force. However, all of the calculated capillary numbers were orders of magnitude below the range of values that have been previously reported for immiscible-liquid mobilization [44]. These results indicate that immiscible-liquid compositional changes did not impact the physical properties sufficiently to mobilize immiscible liquid with groundwater flow.

4.3. Phase Partitioning

The results of the batch immiscible-liquid/aqueous and immiscible-liquid/gas partitioning experiments are presented in Figure 2a. The expected linear partitioning is observed for both systems. The PCE concentrations predicted from Raoult's Law are compared to the measured concentrations in the vapor and aqueous phases in Figure 2b. Minor deviations from ideal behavior as predicted by Raoult's Law are observed, which are due to the structural differences between PCE and the other compounds in the PCE-diesel immiscible-liquid mixture (including aliphatic, aromatic, and polycyclic aromatic compounds). The activity coefficients estimated as deviations from ideal behavior [1] ranged from 0.96 to 1.1 for the immiscible-liquid/aqueous system, and from 0.74 to 0.84 for the immiscible-liquid/gas systems. The deviations from ideal behavior were within the 95% C.I. based on the replicates (i.e. statistically insignificant) for the immiscible-liquid/aqueous system, but they were greater than the 95% C.I. for the immiscible-liquid/gas systems (Figure 2b). These results suggest that PCE partitioning is ideal for the immiscible-liquid/aqueous system, and relatively ideal for the immiscible-liquid/gas system.

4.4. Vapor Extraction Results

The results of the dynamic vapor-extraction experiments are presented in Figure 3. The effluent PCE vapor concentrations through time (pore volumes) for the flow cell containing no porous medium are presented in Figure 3a. The effluent concentrations remained relatively constant at 8.8 mg L^{-1} throughout the approximately 300 pore volumes of flushing. The initial effluent concentration of vapor sampled from the flow cell with porous media was similar to the other flow cell. However, after approximately 50 pore volumes, the effluent concentrations decreased (Figure 3b) to a relatively constant mean concentration (0.44 mg L^{-1}) that was significantly lower than that observed for the flow cell without porous media. The flow rates used for both flow cells were similar (average of 40 to 30 ml min^{-1}), and the interstitial velocities were 77 and 53 cm hr^{-1} for the flow cells without and with porous media, respectively (Table 1).

The mass of PCE removed during vapor extraction was estimated using the average flow rate and the effluent concentrations. The experiment conducted with the flow cell containing no porous medium extended for 34 days, and 31% percent (13 g) of the initial PCE mass was removed. This value is similar to the mass removal (37%) from the immiscible liquid compositional analysis conducted before and after vapor extraction (Table 2). The percent removed for each of the compounds (or groups of compounds with similar molecular weights) ranged from 8 to 63%. The changes in mole fraction for the compounds were insignificant (approximately 2%) because the reductions in concentration for each of the measured compounds were similar (Table 2). These results indicate that PCE evaporation during the flow cell experiments was at steady state, and that mass removal during the experiments did not have a significant impact on the immiscible-liquid composition.

4.5. Vapor Extraction Mass-Transfer Rate Limitations

The effluent concentrations measured during the flow-cell experiments were compared to equilibrium values measured for the batch experiments to evaluate potential mass-transfer rate limitations (Table 1 and Figure 3). The gas-phase concentrations observed for the flow cell containing no porous medium (Figure 3a), which averaged 8.8 mg L^{-1} , were comparable to the batch equilibrium concentrations (9.7 mg L^{-1}). This indicates that partitioning between the gas and immiscible liquid was close to equilibrium, suggesting minimal mass-transfer rate limitation for the flow cell without porous media. However, the effluent concentrations were significantly lower than vapor concentrations at equilibrium with pure PCE, which is 104 mg L^{-1} as determined from batch experiments. Thus, the multicomponent nature of the immiscible liquid limited the overall PCE mass removal.

The steady-state effluent vapor concentrations for the flow cell packed with porous media were significantly lower than the equilibrium value (Figure 3b). Initial effluent concentrations were similar to the batch results; however, there was an exponential decrease in vapor concentration upon initiation of vapor extraction. These lower concentrations suggest the existence of mass-transfer rate limitations between the immiscible liquid and the gas phase. Immiscible liquid was injected (as opposed to mixed into the porous media prior to packing), and the limited volume injected was not sufficient to create a uniform residual distribution. Thus, it is likely that dilution effects associated with the nonuniform immiscible-liquid distribution were primarily responsible for the observed mass-transfer rate limitation. Liang et al. [15] observed similar mass-transfer rate limitation behavior in vapor extraction experiments with nonuniform immiscible-liquid distributions where vapor transport occurred adjacent to, but not through, the immiscible-liquid source zone.

Equation 4 was used to determine k_0 for both flow-cell experiments, and the Sherwood numbers were calculated from the k_0 values using Equation 5 (Table 1). The resultant values are presented in Table 1 with a comparison to Sherwood numbers estimated from the correlation (Equation 7) presented in Wilkins et al. [10]. The Sherwood number and rate coefficient were larger for the flow cell without porous media, which was expected based on the above discussion. The value for the flow cell experiment conducted with porous media is approximately one order of magnitude lower than the value estimated using the correlation. However, the correlation is specific to the experimental conditions used, and does not incorporate multicomponent immiscible liquid or nonuniformly distributed immiscible liquid, which can significantly impact vapor mass transfer.

5. Summary

The results of this investigation have shown that the presence of PCE in an immiscible-liquid mixture does affect the physical properties and the phase-partitioning behavior of the mixture. The phase partitioning was relatively ideal, which allows the use of Raoult's Law to predict

behavior. The results of the flow-cell vapor extraction experiments suggest that evaporation was rate limited for the experiment conducted with the flow cell packed with porous media, which was attributed to a nonuniform immiscible-liquid distribution and dilution effects.

Acknowledgments

This research was supported in part by funding provided by the Arizona Department of Environmental Quality, the U.S. EPA, and the NIEHS Superfund Basic Research Program (P42ES04940). We appreciate the collaboration and assistance of Miller Brooks Environmental and Golder Associates Inc. We would also like to thank Asami Murao for assistance with the GC analysis and Dr. Maier for the use of the Tensiomat.

References

1. McCray JE, Dugan PJ. Nonideal equilibrium dissolution of trichloroethene from a decane-based nonaqueous phase liquid mixture: Experimental and modeling investigation. *Water Resources Research* 2002;38(10):1029-1036. [PubMed: 12000883]
2. Broholm MM, Christophersen M, Maier U, Stenby EH, Hohener P, Kjeldsen P. Compositional evolution of the emplaced fuel source in the vadose zone field experiment at airbase Vaerlose, Denmark. *Environmental Science & Technology* 2005;39:8251-8263. [PubMed: 16294861]
3. Rostad CE, Pereira WE, Hult MF. Partitioning Studies of Coal-Tar Constituents in a 2-Phase Contaminated Groundwater System. *Chemosphere* 1985;14:1023-1036.
4. Borden RC, Kao CM. Evaluation of Groundwater Extraction For Remediation of Petroleum-Contaminated Aquifers. *Water Environment Research* 1992;64:28-36.
5. Whelan MP, Voudrias EA, Pearce A. DNAPL pool dissolution in saturated porous media; procedure development and preliminary results. *Journal of Contaminant Hydrology* 1994;15:223-237.
6. Chen CSH, Delfino JJ, Rao PSC. Partitioning of Organic and Inorganic Components From Motor Oil Into Water. *Chemosphere* 1994;28:1385-1400.
7. Lesage S, Brown S. Observation of the Dissolution of Napl Mixtures. *Journal of Contaminant Hydrology* 1994;15:57-71.
8. Adeel Z, Luthy RG, Dzombak DA. Leaching of PCBs From A NAPL Entrapped In Porous Media. *NAPLs in Subsurface Environment* 1996:649-660.
9. Mukherji S, Peters CA, Weber WJ. Mass transfer of polynuclear aromatic hydrocarbons from complex DNAPL mixtures. *Environmental Science & Technology* 1997;31:416-423.
10. Wilkins MD, Abriola LM, Pennell KD. An Experimental Investigation of Rate-Limited Nonaqueous Phase Liquid Volatilization in Unsaturated Porous-Media - Steady-State Mass-Transfer. *Water Resources Research* 1995;31:2159-2172.
11. Yoon H, Kim JH, Liljestrand HM, Khim J. Effect of water content on transient nonequilibrium NAPL-gas mass transfer during soil vapor extraction. *Journal of Contaminant Hydrology* 2002;54:1-18. [PubMed: 11848263]
12. Anwar AHMF, Tien TH, Inoue Y, Takagi F. Mass transfer correlation for nonaqueous phase liquid volatilization in porous media. *Environmental Science & Technology* 2003;37:1277-1283.
13. Abriola LM, Bradford SA, Lang J, Gaither CL. Volatilization of binary nonaqueous phase liquid mixtures in unsaturated porous media. *Vadose Zone Journal* 2004;3:645-655.
14. Gioia F, Murena F, Santoro A. Transient evaporation of multicomponent liquid mixtures of organic volatiles through a covering porous layer. *Journal of Hazardous Materials* 1998;59:131-144.
15. Liang HL, Udell KS. Experimental and theoretical investigation of vaporization of liquid hydrocarbon mixtures in water-wetted porous media. *Water Resources Research* 1999;35:635-649.
16. Harper BM, Stiver WH, Zytner RG. Nonequilibrium nonaqueous phase liquid mass transfer model for soil vapor extraction systems. *Journal of Environmental Engineering-Asce* 2003;129:745-754.
17. Wang G, Reckhorn SBF, Grathwohl P. Volatile Organic Compounds Volatilization from Multicomponent Organic Liquids and Diffusion in Unsaturated Porous Media. *Vadose Zone Journal* 2003;2:692-701.

18. Garg S, Rixey WG. The dissolution of benzene, toluene, m-xylene and naphthalene from a residually trapped non-aqueous phase liquid under mass transfer limited conditions. *Journal of Contaminant Hydrology* 1999;36:313–331.
19. Roy JW, Smith JE, Gillham RW. Natural remobilization of multicomponent DNAPL pools due to dissolution. *Journal of Contaminant Hydrology* 2002;59:163–186. [PubMed: 12487412]
20. ADEQ. Updated Site Conceptual Model 2001 for Park-Euclid Water Quality Assurance Revolving Fund Site Tucson, Arizona. Arizona Department of Environmental Quality; Tucson: 2001.
21. Banerjee S. Solubility of Organic Mixtures in Water. *Environmental Science and Technology* 1984;18:587–591.
22. Burris DR, MacIntyre WG. Water Solubility Behavior of Binary Hydrocarbon Mixtures. *Environmental Toxicology and Chemistry* 1985;4:371–377.
23. McCray JE, Brusseau ML. Cyclodextrin enhanced in situ flushing of multiple-component immiscible organic liquid contamination at the field scale: Analysis of dissolution behavior. *Environmental Science & Technology* 1999;33:89–95.
24. Borden RC, Piwoni MD. Hydrocarbon Dissolution and Transport - a Comparison of Equilibrium and Kinetic-Models. *Journal of Contaminant Hydrology* 1992;10:309–323.
25. Mackay D, Shiu WY, Maijanen A, Feenstra S. Dissolution of Nonaqueous Phase Liquids in Groundwater. *Journal of Contaminant Hydrology* 1991;8:23–42.
26. Cline PV, Delfino JJ, Rao PSC. Partitioning of Aromatic Constituents Into Water From Gasoline and Other Complex Solvent Mixtures. *Environmental Science & Technology* 1991;25:914–920.
27. Lee LS, Hagwall M, Delfino JJ, Rao PSC. Partitioning of Polycyclic Aromatic-Hydrocarbons From Diesel Fuel Into Water. *Environmental Science & Technology* 1992;26:2104–2110.
28. Lee LS, Rao PSC, Okuda I. Equilibrium Partitioning of Polycyclic Aromatic-Hydrocarbons From Coal-Tar Into Water. *Environmental Science & Technology* 1992;26:2110–2115.
29. Cohen, RM.; Mercer, JW. DNAPL site evaluation. C.K. Smoley; Boca Raton, FL, United States: 1993. p. 314
30. Rivett, MO.; Feenstra, S.; Cherry, JA. Transport of a dissolved-phase plume from a residual solvent source in a sand aquifer. In: Wheeler, HS.; Raats, PAC.; Armstrong, AC., editors. Field, laboratory and modelling studies of flow and transport processes., *Journal of Hydrology*. Vol. 159. Elsevier; Amsterdam, Netherlands: 1994. p. 27-41.
31. Lane WF, Loehr RC. Predicting Aqueous Concentrations of Polynuclear Aromatic-Hydrocarbons in Complex-Mixtures. *Water Environment Research* 1995;67:169–173.
32. Luthy RG, Dzombak DA, Shannon MJR, Unterman R, Smith JR. Dissolution of PCB congeners from an Aroclor and an Aroclor/hydraulic oil mixture. *Water Research* 1997;31:561–573.
33. Broholm K, Feenstra S, Cherry JA. Solvent release into a sandy aquifer. 1. Overview of source distribution and dissolution behavior. *Environmental Science & Technology* 1999;33:681–690.
34. Seagren EA, Rittmann BE, Valocchi AJ. An experimental investigation of NAPL pool dissolution enhancement by flushing. *Journal of Contaminant Hydrology* 1999;37:111–137.
35. Peters CA, Wammer KH, Knightes CD. Multicomponent NAPL solidification thermodynamics. *Transport in Porous Media* 2000;38:57–77.
36. Eberhardt C, Grathwohl P. Times scales of organic contaminant dissolution from complex source zones: coal tar pools vs. blobs. *Journal of Contaminant Hydrology* 2002;59:45–66. [PubMed: 12683639]
37. Rivett MO, Feenstra S. Dissolution of an emplaced source of DNAPL in a natural aquifer setting. *Environmental Science & Technology* 2005;39:447–455. [PubMed: 15707043]
38. Sherwood, TK.; Pigford, RL.; Wilke, CR. *Mass Transfer*. McGraw-Hill; New York: 1975.
39. Powers SE, Abriola LM, Weber WJ. An Experimental Investigation of Nonaqueous Phase Liquid Dissolution in Saturated Subsurface Systems - Steady-State Mass-Transfer Rates. *Water Resources Research* 1992;28:2691–2705.
40. Ng KM, Davis HT, Scriven LE. Visualization of Blob Mechanics in Flow Through Porous-Media. *Chemical Engineering Science* 1978;33:1009–1017.
41. Morrow NR. Interplay of Capillary, Viscous and Buoyancy Forces in the Mobilization of Residual Oil. *Journal of Canadian Petroleum Technology* 1979;18:35–46.

42. Cohen RM, Mercer JW. Review of Immiscible Fluids in the Subsurface: Properties, Models, Characterization and Remediation. *Journal of Contaminant Hydrology* 1990;6:107–163.
43. Dawson HE, Roberts PV. Influence of viscous, gravitational, and capillary forces on DNAPL saturation. *Ground Water* 1997;35:261–269.
44. Larson RG, Davis HT, Scriven LE. Displacement of Residual Non-Wetting Fluid From Porous-Media. *Chemical Engineering Science* 1981;36:75–85.
45. Morrow, NR.; Chatzis, I. Measurement and correlation of conditions for entrapment and mobilization of residual oil. U.S. Department of Energy; Bartlesville, OK: 1981. p. 110
46. Golder. Park-Euclid WQARF Site Well PER-15 Pump Test Analysis Results. Golder Associates Inc.; Tucson, AZ: 2001.
47. Lide, DR.; Frederikse, HPR., editors. *Handbook of Chemistry and Physics*. CRC Press; New York: 1995.

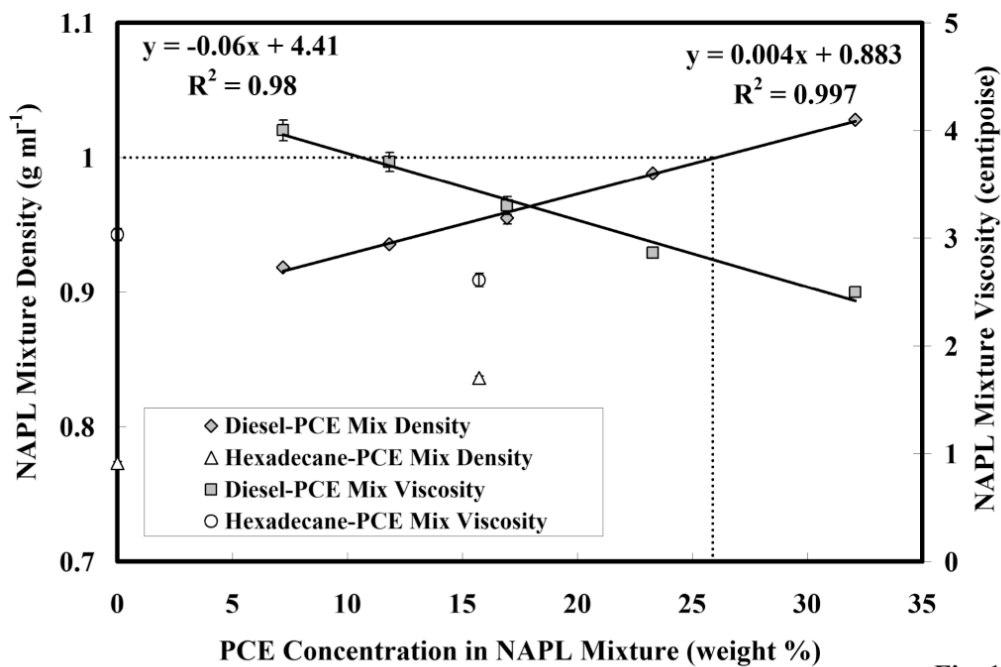


Fig. 1a

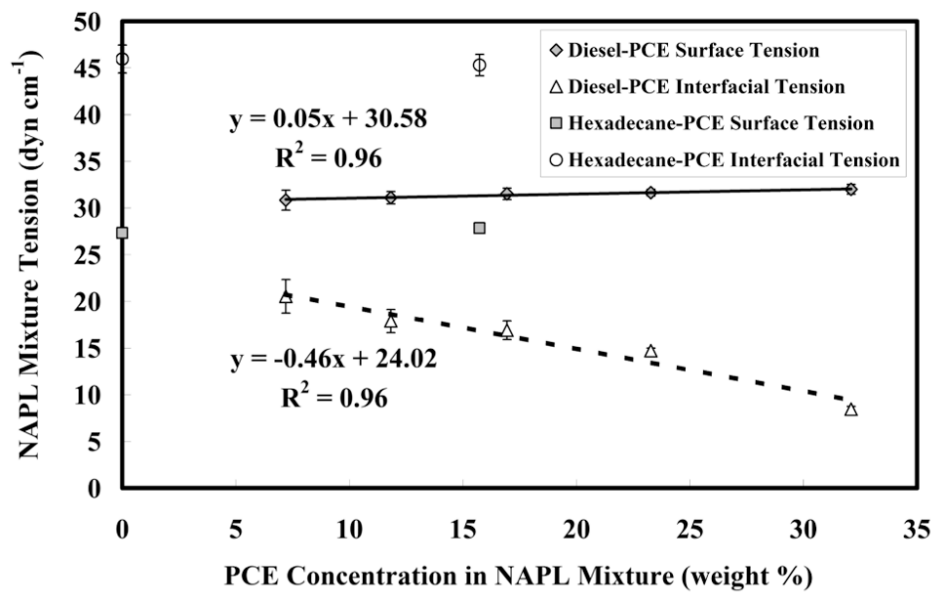


Fig. 1b

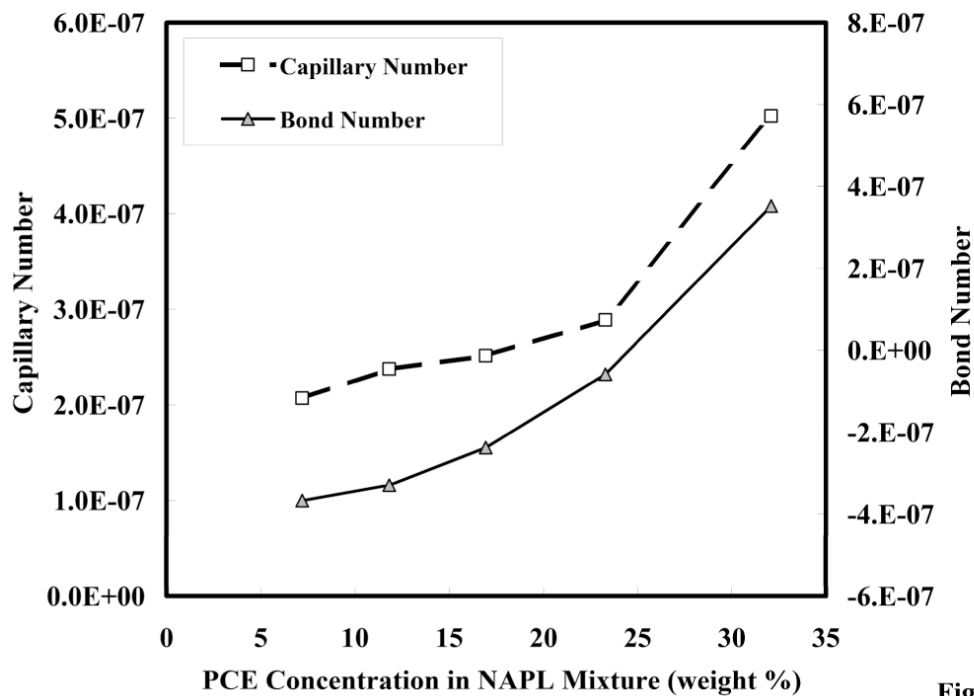


Fig. 1c

Figure 1.

Figure 1a. Density and viscosity of the PCE-diesel immiscible-liquid mixture; error bars calculated from the 95% confidence interval (C.I.).

Figure 1b. Surface and interfacial tension of the PCE-diesel immiscible-liquid mixture; error bars calculated from the 95% C.I.

Figure 1c. Capillary and bond numbers of the PCE-diesel immiscible-liquid mixture.

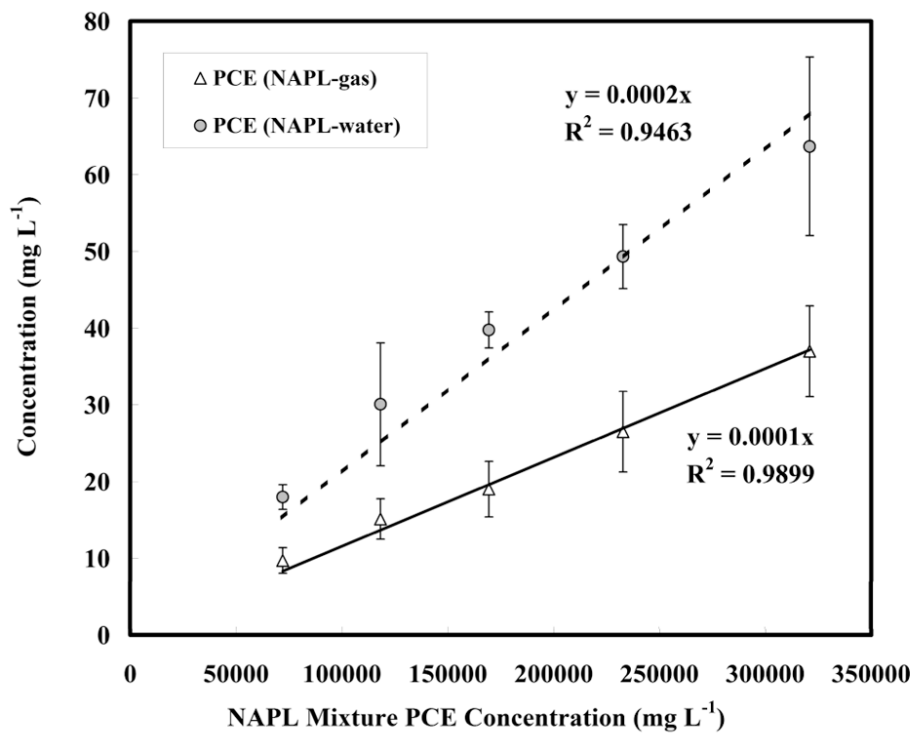


Fig. 2a

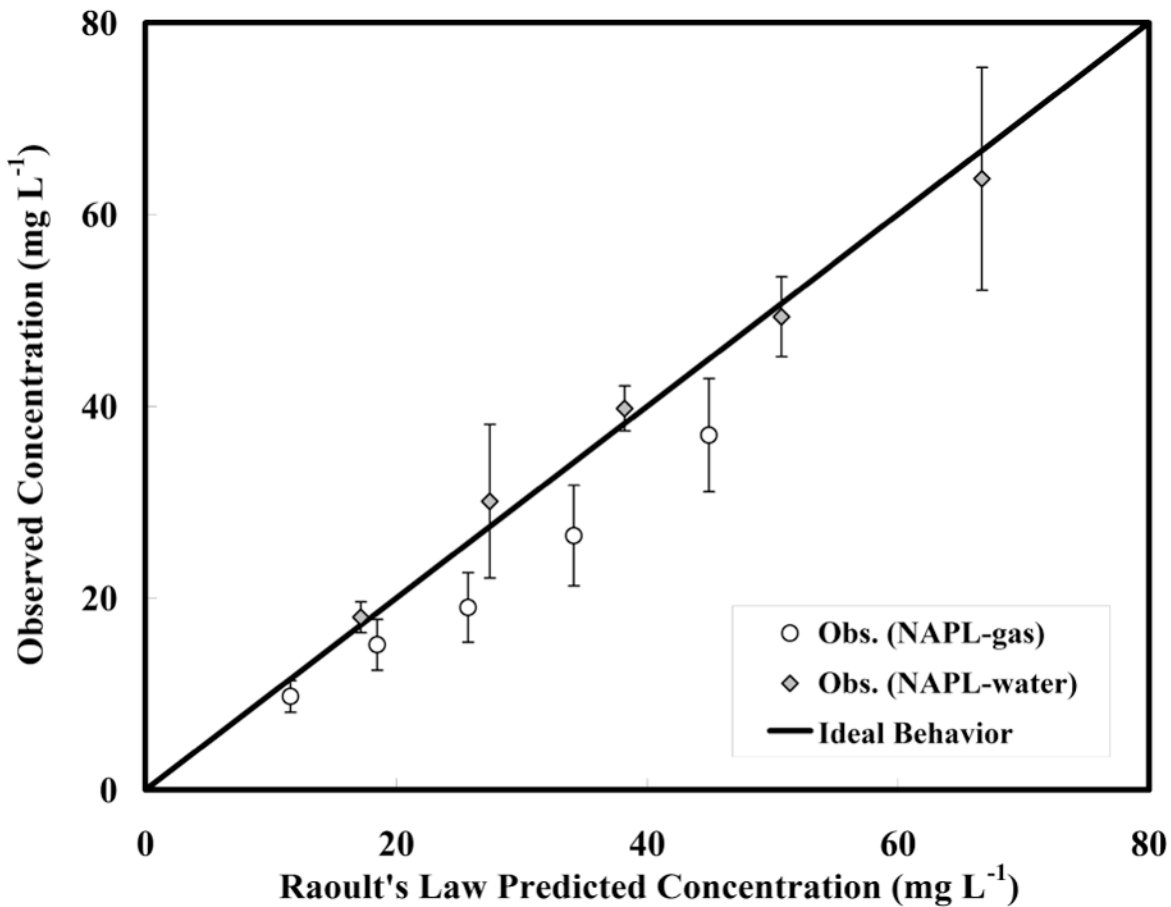


Fig. 2b

Figure 2.

Figure 2a. Equilibrium partitioning behavior of the PCE-diesel immiscible-liquid mixture; error bars calculated from the 95% C.I.

Figure 2b. Raoult's Law prediction and observed PCE partitioning from the PCE-diesel immiscible-liquid mixture; error bars calculated from the 95% C.I.

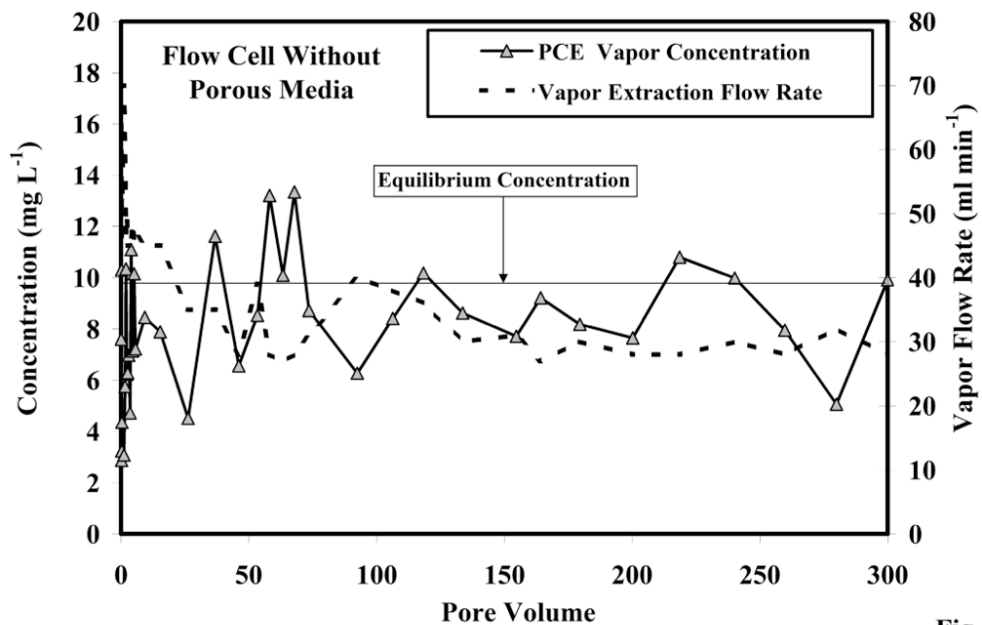


Fig. 3a

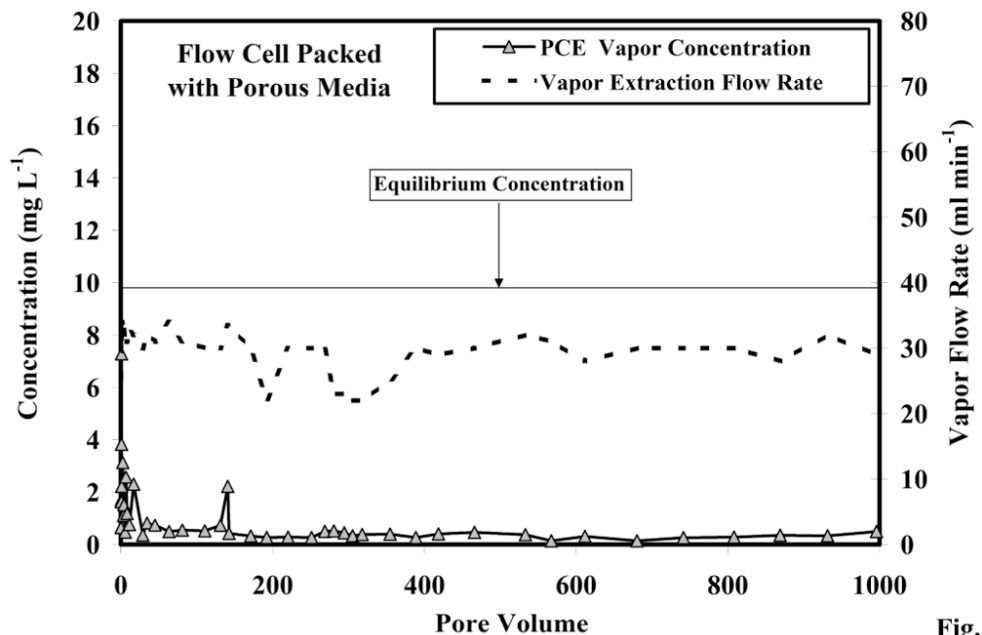


Fig. 3b

Figure 3. Figure 3a. Effluent concentrations, equilibrium concentration, and vapor flow rate comparison for the flow cell conducted without porous media (free-phase immiscible liquid). Figure 3b. Effluent concentrations, equilibrium concentration, and vapor flow rate comparison for the flow cell packed with porous media (free-phase immiscible liquid).

Table 1

Flow cell experimental properties

	Without Porous Media	With Porous Media
Flow Cell Dimensions		
Height (cm)	5.3	5.3
Width (cm)	19.9	19.9
Length (cm)	39.7	39.7
Volume (L)	4.2	4.2
Vapor Extraction Experimental Conditions		
Average Flow Rates (cm ³ min ⁻¹)	40	30
Cross Sectional Area (cm ²)	31.16	105.47
Average Darcy Velocity (cm hour ⁻¹)	77.02	17.07
Average Interstitial Velocity (cm hour ⁻¹)	77.02	53.06
NAPL (L)	0.650	0.075
Water (L)	2.30	0.20
Air (L)	1.24	1.08
Pore Volume (L)	1.24	1.08
NAPL Saturation (-)	0.16	0.06
Water Saturation (-)	0.55	0.15
Air Saturation (-)	0.30	0.80
Mass Removed Through Vapor Extraction		
PCE Mass Removed (g)	13.35	0.74
PCE Removed (% of initial mass)	31.05	14.98
Mass Transfer Rate-Limitation Evaluation		
PCE gas phase diffusion coefficient (cm ² hour ⁻¹)	316.8	316.8
Lumped mass transfer rate coefficient (hour ⁻¹)	4.60	0.02
Peclet number (-)	0.38	0.01
Modified Sherwood number (-)	3.46E-02	2.91E-05
Correlation predicted modified Sherwood number (-)	4.55E-01	1.75E-04
Average concentration at steady state (mg L ⁻¹)	8.81	0.44
Equilibrium concentration (mg L ⁻¹)	9.72	9.72

Table 2

Diesel-PCE composition and mole fraction change from the initial field sample due to vapor extraction without porous media

Chemical ^b	Molecular Weight (g mol ⁻¹)	Initial ^a Concentration (mg Kg ⁻¹)	Initial Molarity (mol Kg ⁻¹)	Initial Mole Fraction (-)	Final ^a Concentration (mg Kg ⁻¹)	Final Molarity (mol Kg ⁻¹)	Final Mole Fraction (-)	Concentration Decrease (% of initial)
PCE	165.83	72,000	0.434	0.099	45,000	0.271	0.061	37.5
TCE	131.39	1,300	0.010	0.002	750	0.006	0.001	42.3
C9	128.25	830	0.006	0.001	310	0.002	0.001	62.7
C10	142.28	2,600	0.018	0.004	1,800	0.013	0.003	30.8
C11	156.31	6,100	0.039	0.009	3,800	0.024	0.006	37.7
C12	170.33	17,000	0.100	0.023	10,000	0.059	0.013	41.2
C13	184.36	49,000	0.266	0.061	23,000	0.125	0.028	53.1
C14	198.38	52,000	0.262	0.060	48,000	0.242	0.055	7.7
C15	212.42	110,000	0.518	0.118	66,000	0.311	0.070	40.0
C16	226.44	100,000	0.442	0.101	68,000	0.300	0.068	32.0
C17	240.47	120,000	0.499	0.114	71,000	0.295	0.067	40.8
C18	254.49	120,000	0.472	0.107	71,000	0.279	0.063	40.8
C19	268.53	88,000	0.328	0.075	51,000	0.190	0.043	42.0
C20	282.55	58,000	0.205	0.047	28,000	0.099	0.022	51.7
C21	296.58	39,000	0.131	0.030	23,000	0.078	0.018	41.0
C22	308.59	25,000	0.081	0.018	14,000	0.045	0.010	44.0
C23	322.62	15,000	0.046	0.011	8,400	0.026	0.006	44.0
C24	338.66	6,900	0.020	0.005	4,300	0.013	0.003	37.7
C25	352.69	2,700	0.008	0.002	1,600	0.005	0.001	40.7
Estimated ^c	227.00	114,570	0.505	0.115	461,040	2.031	0.460	-
Total		1,000,000	4.390	1.000	1,000,000	4.413	1.000	-

^aInitial concentration refers to the field sample, and final refers to the mixture from the flow cell without porous media after 322 pore volumes.

^bC9 through C25 refer to molecules with carbon chain lengths of 9 through 25.

^c10% of initial mass not determined from analysis was assumed to be composed of the average molecular weight of 227 g mol⁻¹.